CONSTRUCTION
E-ISSN: 2785-8731
VOLUME 3, ISSUE 1, 2023, 23 – 39
DOI: https://doi.org/10.15282/construction.v3i1.9053

اونيۏرسيتي مليسيا ڤهڠ
UNIVERSITI MALAYSIA PAHANG

RESEARCH ARTICLE

Structural Design of Field Plate Load Test Equipment to Determine In situ Bearing Capacity and Settlement of Clayey Soil

I. Umaru[1,3]*, B. Alkali[2], M. M. Alhaji[3], M. Alhassan[3], T. E. Adejumo[3] and A. H. Jagaba[1,4]

[1]Department of Civil Engineering, Abubakar Tafawa Balewa University, Bauchi, Nigeria
[2]Department of Mechatronics Engineering, Federal University of Technology, Minna, Nigeria
[3]Department of Civil Engineering, Federal University of Technology, Minna, Nigeria
[4]Department of Civil and Environmental Engineering, Universiti Teknologi PETRONAS, Bandar Seri Iskandar, Perak Darul Ridzuan, 32610, Malaysia

ABSTRACT - The study is to design field-operated plate load test equipment to overcome the problem of predicting bearing capacity and settlement of clayey soil on site using the conventional/traditional methods of short-duration plate load test where a hydraulic jack is used in conducting the test. Ashby's method of material selection was used for the selection of a suitable material for each of the components. The 12 mm thickness was obtained as the minimum safe thickness for the applied load of 500 kg on the lever arm. The I-section frame that support the entire system has sectional modulus of 19.4 cm^3 and 4 mm thickness. The equipment will use a lever arm mechanism to conduct an in-situ test that will take long-duration on clay soil where the dissipation of pore water from the clayey soils takes a longer time to complete as against the current conventional method of plate load test that is in use. The equipment will offer several advantages in terms of cost, reliability, portability, authenticity, and user friendly.

ARTICLE HISTORY
Received : 24th Jan. 2023
Revised : 02nd Mar. 2023
Accepted : 20th Mar. 2023
Published : 27th April 2023

KEYWORDS
Plate load test,
Bearing capacity,
Settlement,
In-situ test,
Soil deformation,

1.0 INTRODUCTION

Plate load testing equipment is an in-situ testing equipment used in determination of in-situ soils bearing capacity [1-3]. Testing of the mechanical properties of soil at field conditions have proven to be more accurate and reliable due to the preservation of the soil structure as against laboratory test which can be affected by sample disturbance [4, 5]. The use of in-situ plate loading tests have been in use over the years to determine the bearing capacity of in-situ soil deposits as well as the settlement of the soils under each of the applied loadings. In almost all the plate loading devices in use over the years, Jack has always been used to apply loading on the device and the deformation recorded for each load application [6]. However, the use of jack for load application cannot give sustained loading for a relatively long period of time thereby making it difficult to allow for pore pressure desipation when the equipment is used on in-situ saturated clay soils [7].

The existing in-situ field plate load tests will give accurate and reliable results for the design of shallow foundations on sandy and silty soils [8,9]. These accuracies cannot be guaranteed on in-situ saturated clay soils due to lack of sufficient time for the pore water to decipate and may give erroneous bearing capacity results [10].

An innovative in-situ field plate loading test device was then conceived with gravity loading which can be applied and sustained for a long period of time to allow for pore water dissipation before the next loading increment [11]. The minimum dimension of plate to be used for in-situ field plate loading device is specified to be 30cm due to pressure bulb that will be generated from the base plate [12]. This minimum size of base plate will affect the magnitude of the weight that will be applied to give substantial applied stress since the weight will be divided by the cross-sectional area of the base plate. Invariably, large applied weight is required which cannot be applied directly without any form of load magnification, hence the introduction of a lever arm. The lever arm was designed and used to magnify the load applied to the device so as to achieve high applied stress [13-16]. The study by [17] which conducted a plate load test on the field where a load was applied to the plate through a hydraulic jack against a heavy kentledge of sandbags, in 5 equal load increments of 100 kPa is a typical example of field plate load test using hydraulic jack for load application. The settlement of the plate during the test was measured at two manually recording dial gauges placed on the plate at diagonally opposite locations on a field. The pressure recorded by the pressure gauge attached to the hosepipe connecting a manually operated hydraulic jack to control the pressure applied to the plate assembly was observed to drop when allowed for some period of time [15, 18]. Assuming a maximum load to be applied to this equipment and all the steel members to be used must be structurally designed to allow it resist loadings without buckling or failure in bending. The aim of this study therefore is to carry out structural design and analysis of all the steel members required to construct this equipment [18].

***CORRESPONDING AUTHOR | I. Umaru** | ✉ Ibrahim_7639@futminna.edu.ng

2.0 METHODOLOGY

2.1 Methods

Figure 1 shows the flow chart used for the structural design of the in-situ plate load test equipment. Design consideration and maximum loading assumptions were made on the chosen concept followed by the material selection, calculations, design analysis and development of the computer aided design (CAD) model as shown in the flow chart.

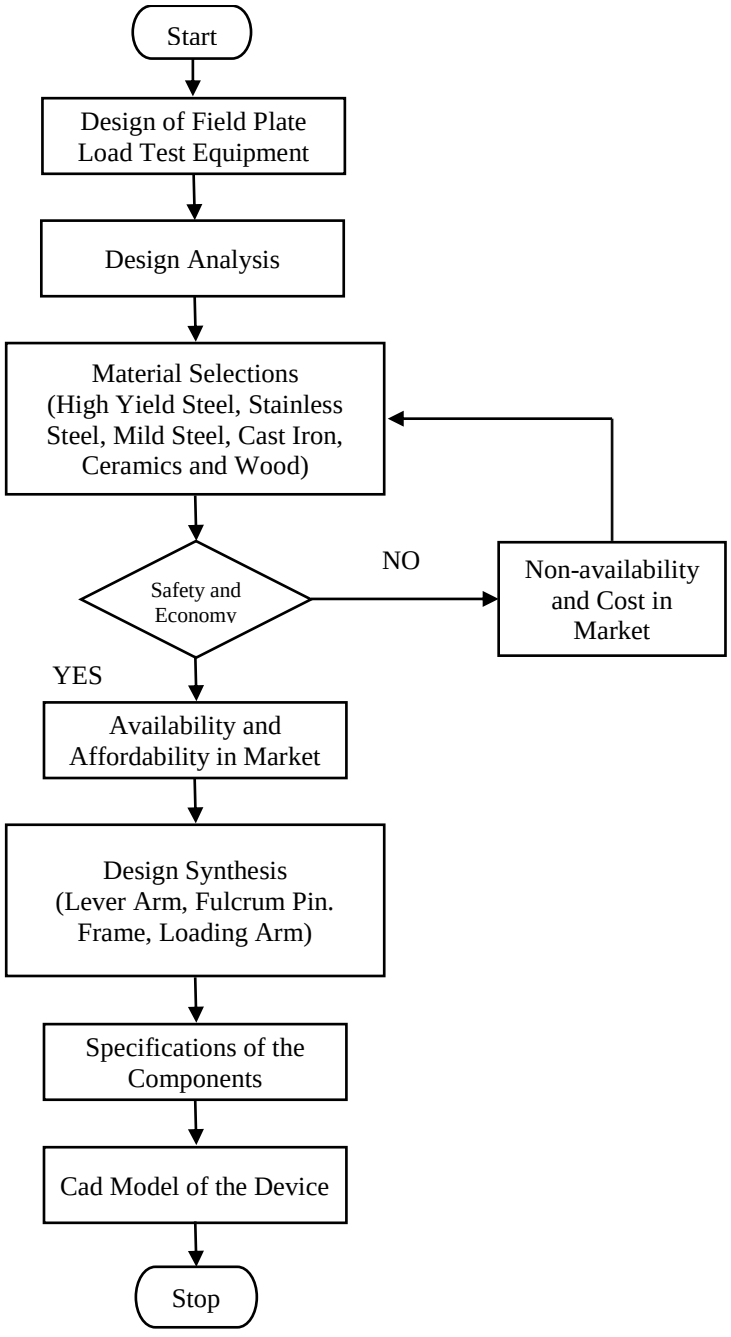

Figure 1. Flow chart of the design

2.2 Material Selections

Ashby's method of material selection was used for the selection of a suitable material for each of the components of the plate load test equipment. The criteria were considered in the following order: material properties, fabricability, availability, and cost of the material. The method uses Young Modulus verse relative cost per volume, strength verse relative cost per volume and Young Modulus verse density, [19]. The focus of the material selection adopted is to make the equipment more cost-effective, meet strength requirements, be light in lightweight and resistant to failure. There are many sources of reliable and consistent data on material properties and other information which includes governmental agencies, trade associations, engineering societies, textbooks, research institutes and material producers [20].

2.3 Description of the Innovative Plate Load Test Equipment

The plate load test equipment shown in Figure 10 is an innovative field in-situ test equipment that is structurally designed and constructed to determine the bearing capacity and settlement of foundation on in-situ saturated clay soils. The equipment uses a straight lever arm mechanism with a parallel force acting in the same plane Figure 2. The equipment will be loaded incrementally through the load hanger known as effort, P attached to the lever arm and balance load W, at the opposite end to produce an equilibrium of weight on a fulcrum which will then be transmitted to the square base plate of dimension 300mm x 300mm and 25mm thick [20]. It has been specified that the load shall be applied in cumulative equal increments up to 1 kg/cm^2 (100 kPa) or $\left({}^1/_5\right)$ of the estimated ultimate bearing capacity. Also, [5] states that the load should be applied in cumulative equal intervals of not more than 1.0 ton/ft^2 (95 kPa) or one-tenth $\left({}^1/_{10}\right)$ of the estimated bearing capacity. However, in this study, the load will be applied at the lever arm through a load hanger in order of 5 kg, 10 kg, 20 kg, 40 kg, 80 kg, 160 kg, and 320 kg as reported by [21] and [5] respectively. This is because the dissipation of pore water pressure from clay soils is gradual and requires slow incremental loadings from smaller to higher loads. Each load placed on the lever arm will be maintained for 24 hours before the next incremental loadings.

2.4 Lever Arm Design

A first-class type of lever mechanism (Figure 2) was used as a lever arm for the plate load test equipment because the fulcrum is located in between the load and the effort. An I-section was used for the lever arm to minimize the twisting along both axes due to the overhand loads. Therefore, the lever arm was designed for strength, rigidity and the dimensions of the lever arm were determined using equations (2-5).

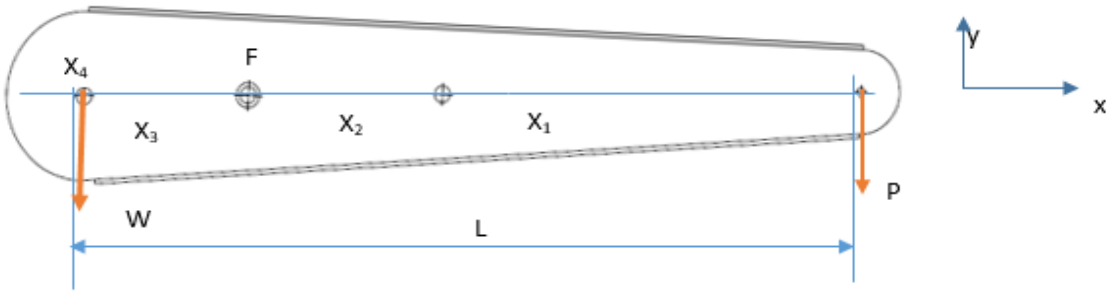

Figure 2. Lever arm

The fulcrum F, is between the load and effort is termed the first type of lever. In this case, effort arm is greater than the load arm.

$$W \times X_1 = P \times L \quad (1)$$

where,
P = Loads (N),
W = balancing load (N),
L= distance from P to the fulcrum F (mm),
X_1 = Distance from Balancing load W to fulcrum (mm).

$$V_1 = L \times B \times t \quad (2)$$

where,
L= length (mm)
B = breath (mm)
t = thickness (mm)
= 516,000 mm^3

From equation 3,

$$V_2 = \frac{1}{2} \times b \times h \times t \quad (3)$$

$= 193{,}500\ mm^3$.

From equation 4,

$$V_3 = {}^1/_2 \times \pi \times B^2 \times t \quad (4)$$

$V_3 = 28{,}865.38\ mm^3$

From equation 4,
V_4=1/2 × π × 20^2 x 15
$= 9{,}242.78\ mm^3$

From equation (2)
V_5 = L× b × t
=322,500 ×2
= 645,000 mm^3

The total volume V of the lever arm is expressed by equation (5) and substituting the values of the V_1, V_2, V_3, V_4, and V_5 gives

$$V = V_1 + V_2 + V_3 + V_4 + V_5 \quad (5)$$

where,
V = total volume (mm^3)
V_1, V_2, V_3, V_4, and V_5 = volume of each components
= 1,392,608.16 mm^3

However, the weight of the lever arm W, equation. (6), is express as;

$$W=rho \times V \times g \quad (6)$$

where,
rho = density γ (kg/m^3)
g = acceleration due to gravity 9.81 kg/m^3
= 11.00 kg

The fulcrum was placed at the distance between effort W and fulcrum F at X_1 = 795 mm and X_2 = 65 mm. The sections and values are tabulated in table 1.

Table 1. Components and values of Lever's arm

S/No.	Sections	Value	Unit
1.	Load, P	500,000	Kg
2.	Load P	5000	N
3.	Length, L	0.915	m
4.	Distance, X_1	0.795	m
5.	Distance, X_2	0.650	m
6.	Distance X_3	0.350	m
7.	Distance X_4	0.200	m
8.	Balancing Weight W	15	Kg

For equilibrium of the lever arm, i.e $\sum m_0 = 0; P \times X_2 = W \times X_1$

5,000 N = 795 mm

And therefore, the moment M, acted on the lever arm equation (7) is express as;

$$M = p \times L \quad (7)$$
$$= 4{,}000{,}000 N/mm$$

According to [22], the sectional modulus of the I-section in Figure 3, was computed using equations (8) and (9). From figure 3, the breath. B and depth, D of the I-section is given by B = 2.5t and D = 6t. Where t, is the thickness.

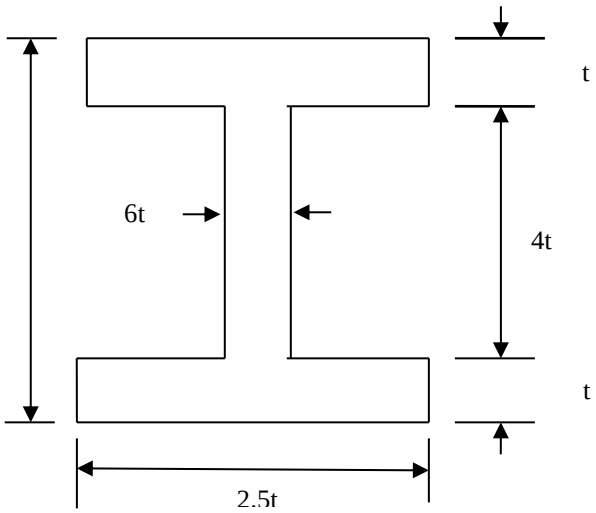

Figure 3. Proportion of I- Section

Therefore, sectional modulus, Z, is given by equation (8) as explain by [22]

$$Z = \frac{I}{(D/_2)} \tag{8}$$

From the proportion of I-section Figure 3, equation (9) was used to determine sectional modulus, Z

$$Z = \frac{\frac{1}{12}[2.5t(6t)^3 - 1.5t(4t)^3]}{\frac{6t}{2}} \tag{9}$$

$Z = 12.3t^3$

The yield stress of mild steel is 220 MPa [22], according to equation (10), bending stress σ_b of the lever arm was obtained as;

$$\sigma_b = \frac{m}{z} \tag{10}$$

where,
M = moment

However, the thickness t, of the lever is calculated from the equation (10)

$$220 = \frac{4{,}000{,}000}{12.3t^3}$$

where,
Thickness t,
$t = \mathbf{12\ mm}$

Therefore, from [23], the I-section ISMB 125 was chosen. The values of the Lever arm section are shown in Table 2.

Table 2. Dimension of lever arm

Sections	Value (units)
Depth of I-section D	125 mm
Thickness t	12 mm

Therefore, the bending stress, σ, for the lever section was computed from equation (10). According to [22] the allowable bending stress, $|\sigma_b|$ is given by equation (11)

$$\frac{4{,}000{,}000}{71800} = \mathbf{56}\frac{\boldsymbol{N}}{\boldsymbol{mm^2}}.$$

$$|\sigma_b| = \frac{\sigma_y}{FS} \quad (11)$$
$$= \frac{56}{2} = 28\ N/mm^2 \qquad \text{is ok.}$$

Therefore, for a factor of safety 2, the maximum bending stress of 28N/mm^2 is below the permissible value of 110 N/mm^2 the design is safe.

2.5 Design for fulcrum

The fulcrum, in Figure 4, is the point at which the lever arm turns relative to the frame of the plate load test equipment. The pin (see Figure 4) at the fulcrum is subjected to a shearing load and therefore, designed using equations (12) and (13). The diameter of a pin was determined from equation (13), and combining equations (12) and (13) yielded equation (14);

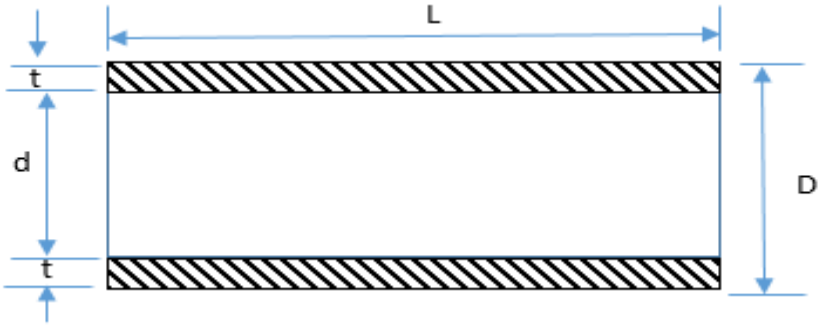

Figure 4. Fulcrum of the lever arm

$$R_f = d \times l\ x\ \sigma_b \quad (12)$$

where,
R_f is Load on fulcrum pin

$$l = 1.25\ d \qquad [22] \quad (13)$$

where,
t=3mm, and L is the length of the pin equation (14).

$$d = \sqrt{\frac{R_f}{z}} \quad (14)$$
$$d = 15mm$$

and the required length of the pin is computed from equation (12). To determine the working stress in the fulcrum, equation (15);

$$l = 1.25 \times 15 = 21\ mm$$

$$\tau = \frac{R_f}{A} \quad (15)$$
$$\tau = 11\ N/mm^2 \text{ ok}$$

A bushing 3 mm thick was inserted in the pinhole. Therefore, the diameter D, of the hole in the fulcrum equation (16). The diameter is taken twice the diameter of the hole L equation (17). Induce bending stress, σ from equation (18),

$$D=d+2xt \quad (16)$$
$$= 23\ mm$$

$$L = 2d \quad (17)$$
$$= 30\ mm$$

$$m = \frac{5}{24} w.l \quad (18)$$
$$= 21{,}875\ Nmm$$

Also, the sectional modulus Z, of the material is given by equation (9). Therefore, the bending induced σ, is expressed by equation (10),

$$Z = \frac{\frac{1}{12}\, x\, l\, [(L)^3 - (d_1)^3]}{l_1}$$
$$= 4{,}012\ mm^3$$

$$\sigma = \frac{m}{Z}$$
$= 5.45\ N/mm^2$ is <220N/mm^2

The induce bending stress | σ |**,** is within safe limits, yielding stress equation (11) is calculated as;

$$|\sigma| = \frac{\sigma_h}{FS}$$
$= 2.725\ N/mm^2$ is ok.

2.6 Design for the pin at fulcrum and loading arm pin

The fulcrum pin connects the lever arm and the load transfer column through a revolute joint. Therefore, the pin is subjected to shearing stress as shown in Figure 5. And the pin load is given by equation (18). While equations (19), (20), and (21) are for the length of the pin, maximum bending moment, and sectional modulus of the materials respectively.

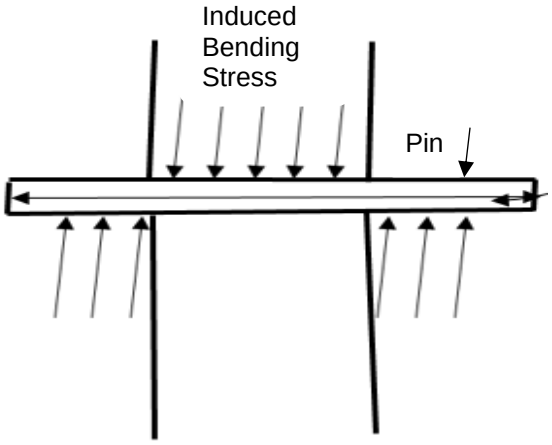

Figure 5. Pin at the fulcrum

$$P = d_1 \times l_1 x\, p_b \tag{19}$$

If the pin is going to fail due to the bearing of the pin of the fulcrum, then the pin diameter is determined by equation (19). From equation (13),

$d_1 = 27\ mm.$
$l_1 = 1.25\ d_1 = 34\ mm$.
$l = 1.25\ d$
$= 34\ mm$

However, from equation (12), the shear stress on fulcrum pin is determined as

$$R_f = 2 \times \frac{\pi}{2} \times d^2 \times \tau$$
$$\tau = 4\ N - mm^2$$

Since the end is forked and therefore the thickness of each eye, equation (20), The inner diameter of each eye, D.

$$t_1 = \frac{l_1}{2} \tag{20}$$
$t_1 = 17\ mm$
$d_1 + 2 \times 3 = 33\ mm$
$D = 2d_1 = 54\ mm$

The maximum bending moment on the fulcrum pin at Y-Y, from equation (21), and the sectional modulus of the fulcrum section is given in equation (22). Bending stress-induced, from equation (9).

$$m = \frac{w}{2}\left(\frac{l_1}{2} + \frac{l_1}{3}\right) - \frac{w}{2} \times \frac{l_1}{4} = \frac{5}{24}\, w\, x\, l_1 \tag{21}$$

$$= 34{,}416.66\ Nmm$$

$$Z = \frac{\pi}{32}(d_1)^3 \tag{22}$$

$$= 1{,}932.37\ mm^3$$

$$\sigma_b = \frac{m}{z} = 18\ MPa \text{ ok}$$

3.0 DESIGN OF THE FRAME

The frame is an assembly where the lever arm and the load are placed, the frame consists of I-beam and I-section column. The load is transferred to the crossing beam and in turn, transferred to the column as shown in Figure (10).

3.1 Design of crossing beam

The cross beam is used to support the load from the lever arm and transfer it to the column. It is designed using equation (23) and is shown in Figure 6. The proportion of the support beam is taken as t = thickness, h = depth as 5t. The result is shown in Table 3. Moment of inertial I, [24] equation (23). The Sectional Modulus Z, is calculated using equation (24)

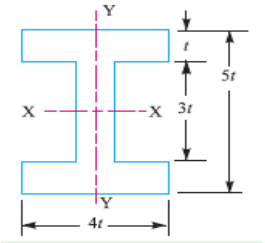

Figure 6. Proportioning of the crossing beam

$$I = \frac{1}{12}[BxD^3 - bxd^3] \tag{23}$$

$$I_{xx} = \frac{1}{12}[4t\ (5t)^3 - 3t(3t)^3] = \frac{419}{12}t^4\ mm^4$$

$$I_{yy} = \left[2x\frac{1}{12}tx(4t)^3 + \frac{1}{12}3txt^3\right] = \frac{131}{12}t^4\ mm^4$$

$$Z = \frac{I_{xx}}{\frac{5t}{2}} \tag{24}$$

$$= 13.97t^3.$$

From [22], the yield stress of mild steel was taken as 220 Mpa. The thickness of the load transfer column was estimated using equation (9),

$$\sigma_b = \frac{m}{Z}$$

$$Z = 18{,}181.18\ mm^3 = 18.18\ cm^3$$

From [23] The I-section chosen for the crossing beam is ISLB 75 is presented in Table 3.

Table 3. Dimension of the selected section

Sections	Value (units)
Depth of I-section	75.00 mm
Breath	50.00 mm
The thickness of web t_w	3.70 mm
The thickness of flanges t_f	5.00 mm
Area of section A	7.71 cm^2
Sectional Modulus Z_{xx}	19.40 cm^3

3.2 Load transfer column

The load transfer column is a slender column attached to the fulcrum that transfers the dead load to the base of the foundation. The load transfer column is shown in Figure 7. Using Euler's method to design for the cripple load as shown in equations (25), (26), and (27). Shear stress at equation (33) and the results are shown in Table 4.

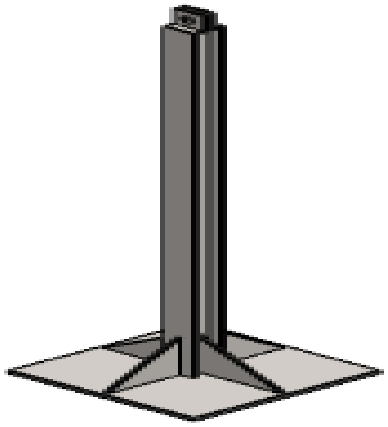

Figure 7. Load transfer column attached with base plate

Area of the section, A =LxB (25)
A = 2(4txt) + 3t x t =$11t^2$

The moment of inertial in the X-axes, $I_{xx,}$ and the Moment of inertia in the Y-axes, $I_{yy,,}$ for the transfer column **is** given below,

$$I_{xx} = \frac{1}{12}[4t\ (5t)^3 - 3t(3t)^3] = \frac{419}{12}t^4\ mm^4$$

$$I_{yy} = \left[2x\frac{1}{12}tx(4t)^3 + \frac{1}{12}3txt^3\right] = \frac{131}{12}t^4\ mm^4$$

Therefore,

$$\frac{I_{xx}}{I_{yy}} = \frac{419}{131} \times \frac{12}{131} = 3.2$$

Since the value of I_{xx}/I_{yy} lies between 3 and 3.5. The I-section is quite satisfactory [22].
The cripple loadW_{cr}, on the column, steady load [22] equation (26)

$$W_{cr} = fs\ \times\ W$$
=20,000 kN (26)

According to Euler's formula, crippling load $(W_{cr,})$ equation (27). Also, Equation (28), cripple stress, $\sigma_{cr.}$ is expressed below.

$$W_{cr} = \frac{\pi^2 xExI}{L^2}$$
= 5 mm (27)
σ_{cr} = 330 MPa = 330 N/mm^2.

$$\sigma_{cr} = \frac{m}{z}$$
Z= 11816.59 mm^3 = $11.82cm^3$ (28)

However, [23]. The I-section chosen for the column is ISLB 75. As shown in Table 4.

Table 4. Dimension of section

Sections	Value (units)
Depth of I-section	75.00 mm
Breath	50.00 mm
The thickness of web t_w	3.70 mm
The thickness of flanges t_f	5.00 mm
Area of section A	7.71 cm^2
Sectional Modulus Z_{xx}	19.40 cm^3

Consider the moment of inertia for both axes. The radius of gyration K_{xx} and K_{yy} [24] is given in equations (29) and (30)

$$I_{xx} = \frac{1}{12}[4t\ (5t)^3 - 3t(3t)^3] = 8{,}938.667\ mm^4$$

$$I_{yy} = \left[2x\frac{1}{12}tx(4t)^3 + \frac{1}{12}3txt^3\right] = 2{,}794.667\ mm^4$$

$$K_{xx} = \sqrt{\frac{I_{xx}}{A}} = 7.127 \tag{29}$$

$$k_{yy} = \sqrt{\frac{I_{yy}}{A}} = 3.985 \tag{30}$$

The least radius of gyration of the section is considered. However, K_{xx} is the least radius of gyration hence used in equation (28). The effective length of fixed and pinned end le, equation (31) and slenderness ratio λ, [24] equation (32).

$$l_e = \frac{L}{2} = l_e = 1{,}000 \text{ mm} \tag{31}$$

$$\lambda = \frac{le}{K_{(min)}} = 351 \tag{32}$$

$\lambda = 351 \geqq 80$

Hence the column is designed as a long column. However, since the column is fixed, the effective length is l_e,

$=, \frac{L}{2} = 2{,}000 \text{ mm}/2 = 1{,}000 \text{ mm}$

Shear Stress τ, [24] for load transfer column equation (33)

$$\tau = \frac{F}{A} = 7\ N/mm^2 \leqq 220 \text{ N/mm}^2. \text{ Hence the design is ok} \tag{33}$$

3.3 Design of anchor leg

The anchor legs were made from an I-section figure 8, with the crushing stress of $\sigma_{cr} = 330\ Mpa$ [22].

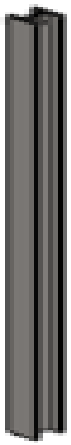

Figure 8. Anchor column legs

Area of the cross-section, A of I-section can be obtained using the equation (25). While, the moment of inertial in the X-axis, $I_{xx,}$ and the moment of inertia in the Y-axis, I_{yy}

$A = 2(4txt) + 3t \times t = 11t^2$

$$I_{xx} = \frac{1}{12}[4t\ (5t)^3 - 3t(3t)^3] = \frac{419}{12}t^4\ mm^4$$

$$I_{yy} = \left[2x\frac{1}{12}tx(4t)^3 + \frac{1}{12}3txt^3\right] = \frac{131}{12}t^4\ mm^4$$

Therefore,

$$\frac{I_{xx}}{I_{yy}} = \frac{419}{131}x\frac{12}{131} = 3.2$$

Since the value of I_{xx}/I_{yy} lies between 3 and 3.5. The I-section is quite satisfactory [22]. The cripple load W_{cr}, on the column, from equation (26) and equation (27), according to Euler's formula, crippling load $(W_{cr,})$

$W_{cr} = fs \times W$
=20,000 kN

$$W_{cr} = \frac{\pi^2 \times E \times I}{L^2}$$
$= 6$ mm

From equation (28)

.σ_{cr} = 330 MPa = 330 N/mm^2.
$\sigma_{cr} = \frac{m}{z}$.
Z= 11.82 cm^3

However, [23]. The I-section chosen for the column is ISLB 75. As shown in Table 5.

Table 5. Dimension of section Anchor Column leg

Sections	Value (units)
Depth of I-section	75 mm
Breath	50 mm
The thickness of web t_w	3.7 mm
The thickness of flanges t_f	5.0 mm
Area of section A	7.71 cm^2
Sectional Modulus Z_{xx}	19.4 cm^3

Consider the moment of inertia for both axes. The radius of gyration K_{xx} and K_{yy} from equation (29) and equation (30). The least radius of gyration of the section is considered. However, K_{xx} is the least radius of gyration hence used in equation (31)

$$I_{xx} = \frac{1}{12}[4t\ (5t)^3 - 3t(3t)^3] = 8{,}938.667\ mm^4$$

$$I_{yy} = \left[2x\frac{1}{12}tx(4t)^3 + \frac{1}{12}3txt^3\right] = 2{,}794.667\ mm^4$$

$$K_{xx} = \sqrt{\frac{I_{xx}}{A}}$$
$$= 7.127$$

$$k_{yy} = \sqrt{\frac{I_{yy}}{A}}$$
$$= 3.985$$

$l_e = \frac{L}{2}$
= 1,500 mm

Slenderness ratio λ, from equation (32)

$$\lambda = \frac{le}{K_{(min)}}$$
$$\lambda = 376.41$$
λ=376.41 ≧80

Hence the column is designed as a long column. However, since the column is fixed, the effective length is $l_e = \frac{L}{2}$= 1,500 mm.

Shear Stress τ, from equation (33),

$$\tau = \frac{F}{A}$$
$\tau = 7\ N/mm^2$ ≦ 220 N/mm^2. Hence the design is ok

3.4 Design of loading arm

The loading arm is made up of mild steel with a circular cross-section and attached to the lever arm. The area of the loading arm was calculated using equation (34) and diameter d,

$$p = \frac{\pi}{4}d^2\sigma_b \quad (34)$$
$$d = 6\ mm$$

Safe tensile load = 28.94 x 220 = 6,366 N

3.5 Design of loading arm pin

The loading arm pin is calculated using equation (19). Let's consider failure due to the bending of the pin at the loading arm and check for shear stress, from equation (15)

$$P = d_1\ \times\ l_1 x\ p_b$$
$$d_1 = 26\ mm$$
$$l_1 = 1.25\ d_1 = 32.5\ mm$$
$$R_f = 2x\tfrac{\pi}{4} \times d^2\tau$$
$\tau = 4.71\ MPa\ is\ ok$t according to [22]

Since the end is forked and therefore the thickness of each eye from equation (20). The inner diameter of each eye, d_1, The maximum bending moment at Y-Y, from equation (21), and Sectional modulus from equation (22). The bending stress induced from equation (10)

$$t_1 = \frac{l_1}{2} = 17\ mm$$

$$d_1 + 2 \times 3 = 32\ mm$$

$$D = 2d_1 = 52\ \ mm$$

$$m = \frac{w}{2}\left(\frac{l_1}{2} + \frac{l_1}{3}\right) - \frac{w}{2} \times \frac{l_1}{4} = \frac{5}{24} \times\ w$$

where,

$$= 33{,}854.178\ Nmm$$

$$Z = \frac{\pi}{32}(d_1)^3$$

$$= 1725.52\ mm^3$$

$$\sigma_b = \frac{m}{z} =\ 19.62\ MPa$$

4.0 RESULTS AND DISCUSSIONS

The conventional methods of conducting plate load tests presented in figure 9 use a hydraulic jack to apply pressure to the soil except figure 9f which uses laboratory-based plate load tests. The reaction plate load test uses a truss to serve as canter load is placed above the pit and hydraulic jack is placed at the bottom of the pit and pressure is applied to the truss through the hydraulic jack figure 9a. A gravity plate load test uses sand bag arrange in a platform to provide for canter weight while a hydraulic jack is placed at the bottom of the pit and pressure is applied through the hydraulic jack figure 9b. A truckload is equally used to conduct a plate load test on a pit with a hydraulic jack placed at a pit and pressure applied through the hydraulic jack which will cause deformation or settlement of the soil figure 9c. [25] uses 1.3 tons of reaction beam with 200kN tons hydraulic jack in conducting plate load test on the field figure 9d. Also, [26] conducted plate load tests on the field with the plate load test equipment they developed using an automatic hydraulic jack (see Figure 9e). while laboratory plate load test was conducted using a lever arm in place of a hydraulic jack but the sampling of undisturbed samples for the test was his major challenge (see Figure 9f). The hydraulic jack used for the test described in figure 9 does not sustain the applied pressure for so long [27]. The drop-in pressure from the hydraulic jack will affect the result obtained from the conventional plate load test which will lead to either under design or overdesign of the intended structure.

(a) (b)

Figure 9. The conventional Plate Load Test Equipment. (a) Reaction loading on test pit [28]
(b) Gravity plate load setup [29],

(c)

(d)

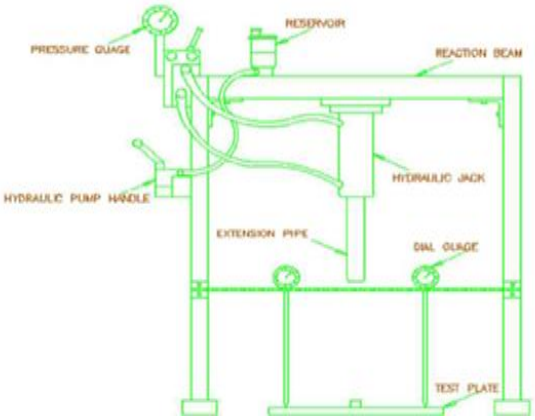

(e)

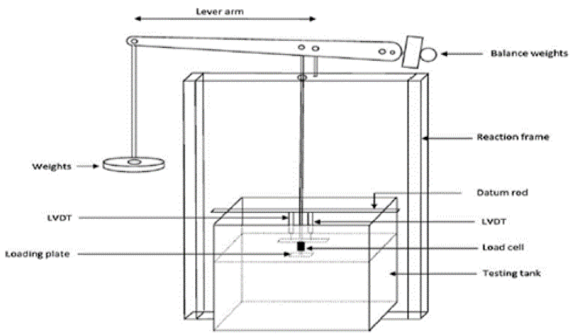

(f)

Figure 9. (cont.) (c) Plate Bearing Test [30], (d) Plate load setup of reaction Beam [25] (e) Schematic of the Plate Load Test Setup [26]. (f) Laboratory Plate Load Test Set-up with Lever Arm [27]

4.2 Sectional modulus of the mechanism

The need for the design of equipment that will not use the hydraulic jack on site on a low permeable clay soil was conceived. The equipment will be very easy to handle and will not require many manpower to operate. Unlike the conventional plate load test equipment in figure 9, this test can be conducted on a developed area where it cannot be accessed by other methods of plate load test equipment

The components of the machine were designed for strength and rigidity. The strength of mild steel used in construction of machine parts that will perform the desired function within the allowable working stress [22]. For each of the components, the minimum fail-safe dimension was determined using strength conditions. Sectional modulus is a direct measure of the strength of a beam or column. For the lever arm, a load of 500 kg was applied and a 12 mm thickness was computed as the minimum stress thickness a similar trend was observed [31]. However, sectional modulus was calculated for beams, transfer column and anchor leg for the entire frame as 19.4 cm^3. The sectional modulus was used in selecting the thickness of web and flanges as 4 mm and 5 mm respectively [23]. The complete Cad model of the field plate load test equipment designed is presented in figure 10.

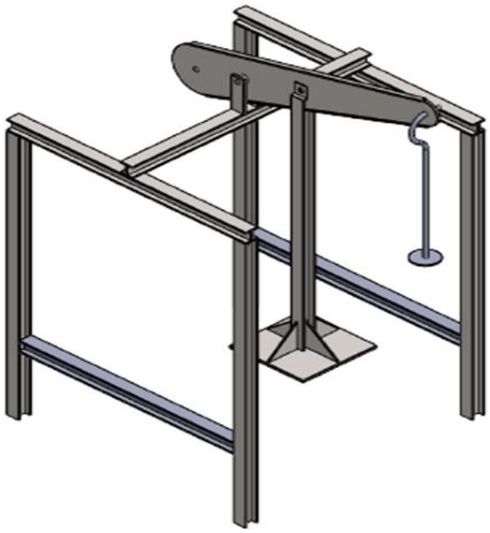

Figure 10. CAD model of field plate load test device

4.3 Shear stress of the components

Shear stress is the strength of component against the type of yield when the component fails in shear. A shear load is a force that tends to produce a sliding failure on a material along a plane that is parallel to the direction of the force. Shear strength of a components is important for designing the dimensions to be used for the construction of machine components or parts. The minimum thickness of lever arm of 12 mm will induce a maximum bending stress of 56 N/mm^2, while crossing beams, transfer column and anchor legs will induce a maximum bending stress of 7N/mm^2 which is less than the bending stress of 220 N/mm^2 [22]. Hence the design is safe to carry the load of 500 kg [32]. The fulcrum pin diameter was designed to be 27 mm with a maximum induced shear stress of 4N/mm^2. Based on the detailed design analysis, the body of the machine could be produced from a C-section having a minimum thickness of 5 mm if the maximum load will not exceed 500 Kg [23].

5.0 CONCLUSION

The plate load test equipment described in this paper was designed to standard. All the steel component members were design, analyzed and observed to resist maximum loading during testing without deformation or failure of any of the steel members. The analysis was used for the final development of the plate load test equipment as an alternative to the existing plate load test equipment that uses a hydraulic jack which has been in use for measuring the in-situ bearing capacity and settlement of soil deposits. In conclusion, the equipment is portable when compare with the existing one and will have high advantage when used on saturated clay deposits as it will allow for maximum deformation after dissipation of pore water pressure for each load application before increment of next loading.

6.0 AUTHOR CONTRIBUTIONS

Ibrahim Umaru.: Conceptualization, Methodology.

Babawuya Alkali.: Data curation, Writing- Original draft preparation.

Mustapha Mohammed Alhaji.: Methodology, Investigation.

Musa Alhassan.: Writing- Reviewing and Editing.

Taye E. Adejimu.: Supervision, Visualization.

Ahmad Hussaini Jagaba.: Software, Formal Analysis.

All authors have read and agreed to the published version of the manuscript.

7.0 FUNDING

Not applicable.

8.0 DATA AVAILABILITY STATEMENT

The data used to support the findings of this study are included within the article.

9.0 ACKNOWLEDGEMENT

The authors gratefully acknowledged the assistance received during the conduct of this research work from the Federal University of Technology, Dadson Engineering Services and Synchronous Logic Engineering in Minna, Niger State, Nigeria.

10.0 CONFLICTS OF INTEREST

The authors declare no conflict of interest.

11.0 REFERENCES

[1] N.C. Consoli, F. Schnaid, and J. Milititsky, "Interpretation of Plate Load Tests on Residual Soil Site," *Journal of Geotechnical and Geoenvironmental Engineering,* 124(9), 857–867, 1998.

[2] Q. Al-Obaidi, A. Al-Shamoosi, and A. Ahmed, "Evaluation of Soil Bearing Capacity by Plate Load Test," P*roceedings of 10th International Conference on the Bearing Capacity of Roads, Railways and Airfields*, Taylor & Francis Group, London, 767-772, 2017.

[3] A. Bubpi, and and P. Poungchompu, "A Field Study on Settlement of Shallow Foundation on Clayey Sand," *KKU Research Journal (Graduate Studies),* 22(2), 130-142, 2022.

[4] BS 1377 (1990). *Methods of testing soil for civil engineering purposes*. British Standards Institute London.

[5] ASTM D1194-94, Standard Test Method for Bearing Capacity of Soil for Static Load and Spread Footings. *Annual book of ASTM standard. American Society for Testing Materials*, Philadelphia, USA, 2003.

[6] I. Umaru, M.M. Alhaji, M. Alhassan, T.W.E. Adejumo, and A. Babawuya, "Evaluation of Load-Settlement Probe Mechanisms: A Review," *2nd International Civil Engineering Conference*. 1(2) 506 -519, 2020.

[7] FM 5-527 Non-repetitive Static Plate Load Test of Soils and Flexible Pavement Components. Florida Department of Transportation. State Materials Office 5007 NE 39th Avenue Gainesville, Florida 32609. 1-8, 2000.

[8] W.T. Oh, and S.K. Vanapalli, "Scale effect of plate load tests in unsaturated soils," *International Journal of Geometry, Geotechnical Material and Environment*, 4 (2) 585-594. ISSN 2186-2983 (P), 2186-2990 (e). Japan, 2013.

[9] M. Omar, "Field Plate Load Test to Investigate Stress Distribution in Soil Mass with and without Reinforcement - United Arab Emirates," *Jordan Journal of Civil Engineering*, 11(4): 623-637, 2017.

[10] Y. Gül, and A. Ceylanoğlu, "Evaluation of Plate Loading Tests on Some Rock Formations for Assessing the Ground Bearing Capacity," *Bulletin of Engineering Geology and the Environment*, 72, 131-136, 2013.

[11] I.S. Samir, "The Assessment of the Collapse Potential of Fills during Inundation using Plate Load Tests," *Life Science Journal*, 11(8):1001-1006 (ISSN: 1097-8135), 2014.

[12] B.B. Tuse, A.B. Lokande, V.R. Ghane, D.D. Parkhe, and C.A. Birajdar, "Investigation of Bearing Capacity by Plate Load Test - A Case Study," *International Conference on Recent Innovation in Science, Engineering, and Technology*, 1-4, 2017.

[13] A.H. Jagaba, S.R.M. Kutty, I.M. Lawal, N. Aminu, A. Noor, B.N.S. Al-Dhawi, A.K. Usman, A. Batari, S. Abubakar, A.H. Birniwa, et al. "Diverse sustainable materials for the treatment of petroleum sludge and remediation of contaminated sites: A review," *Cleaner Waste Systems*, 2, 100010, 2022.

[14] N.R. Mohite, and S. Admane, "Plate Load Test on Undisturbed Soil Sample," *International Journal of Science, Engineering and Technology Research*, 4(4), 1042-1045, 2015.

[15] D.A.M. Araujo, C.M.L. Costam, and Y.D.J. Costam, "Dimension Effect on Plate Load Test Results," *Proceedings of the 2nd World Congress on Civil, Structural and Environmental Engineering*, 1-6, 2017.

[16] A.A. Jawad, R.R. Almuhanna, and A.M. Shaban, "Three-dimensional Finite Element Analysis for Determining Subgrade Reaction Modulus of Subgrade Soils," *IOP Conference Series: Materials Science and Engineering*, 745, 012137. 1-20, 2020.

[17] S.M. Dasaka, "Risk Analysis of Bearing Capacity of Shallow Foundations," Workshop on Emerging Trends in Geotechnical Engineering (ETGE 2012) 8th June 2012, Guwahati, 89-97, 2012.

[18] N.S.A. Yaro, M.H. Sutanto, N.Z. Habib, M. Napiah, A. Usman, A.H. Jagaba, and A.M. Al-Sabaeei, "Application and circular economy prospects of palm oil waste for eco-friendly asphalt pavement industry: A review," *Journal of Road Engineering*, 2 (4), 309-331, 2022.

[19] A. Jagaba, S. Kutty, G. Hayder, L. Baloo, A. Noor, N. Yaro, A. Saeed, I. Lawal, A. Birniwa, and A. Usman, "A Systematic Literature Review on Waste-to-Resource Potential of Palm Oil Clinker for Sustainable Engineering and Environmental Applications," *Materials*, 14, 4456, 2021.

[20] M.M. Farag, *Handbook of Materials Selection*, Edited by Myer Kutz, John Wiley & Sons, Inc., New York. ISBN 0-471-35924-6, 2002.

[21] IS: 1888-2003: Indian Standard Practice on Method of Load Test Standards on soils, Bureau of Indian

[22] R.S. Khurmi, and J.K. Gupta, A Textbook of Machine Design, 1st Multicolor Edition, Eurasia Publishing House (PVT) LTD, New Delhi – 110055, 2008.

[23] BS 5950 2 :(2001) Structural use of steelwork: Specification for materials, fabrication, and erection Rolled and welded sections. British Standards Institute. London.

[24] A.H. Jagaba, A. Shuaibu, I. Umaru, S. Musa, I.M. Lawal, and S. Abubakar, "Stabilization of Soft Soil by Incinerated Sewage Sludge Ash from Municipal Wastewater Treatment Plant for Engineering Construction," *Sustainable Structures and Materials*, 2, 32–44, 2019.

[25] H.F.T. Barnard, and G. Heyman, "The Effect of Bedding Errors on the Accuracy of Plate Load Tests," *Journal of the Civil Engineering*, 57(1), 1-23, 2015.

[26] N.S.A. Yaro, M. Napiah, M.H. Sutanto, A. Usman, I.K. Mizwar, and A.M. Umar, "Engineering Properties of Palm Oil Clinker Fine-Modified Asphaltic Concrete Mixtures, *Journal of Engineering Technological Sciences*, 54 (2), 2022.

[27] S.M. Dasaka, A. Jain, and Y.A. Kolekar, "Effect of Uncertainties in the Field Load Testing on the Observed Load-Settlement Response," *Indian Geotechnical Journal*, 44(3), 294-304, 2013.

[28] P. Sultana, and A.K. Dey, "Estimation of Ultimate Bearing Capacity of Footings on Soft Clay from Plate Load Test Data Considering Variability," *Indian Geotechnical Journal*, 49, 170–183, 2018.

[29] B.B. Tuse, A.P. Path, and D.D. Parche, "Compilation of Plate Bearing Test Data," *International Journal of Advances in Science Engineering and Technology*, 4(4)74-77, 2016.

[30] A.S. Mohammed, "Evaluation of Allowable Bearing Capacity of Soil by Plate Bearing Test. A Case Study in Al-diwaniyah City, *Basrah Journal for Engineering Science,* 101-111, 2013.

[31] A. Ramesh, P. Karunaker, and L. Ramesh, "Design and Analysis of Discharging of Dust in Pneumatic Conveyor System by screw Conveyor Shaft," *Advance Research and Innovations in Mechanical, Material Science, Industrial Engineering and Management – ICARMMIE,* 84-91. Bonfring, 2014.

[32] A.H. Jagaba, S.R.M. Kutty, I.M. Lawal, A.H. Birniwa, A.C. Affam, N.S.A. Yaro, A.K. Usman, I. Umaru, S. Abubakar, A. Noor, "Circular economy potential and contributions of petroleum industry sludge utilization to environmental sustainability through engineered processes—A review," *Cleaner and Circular Bioeconomy*, 3, 100029, 2022.